Article

Tunable THz Pulses Generation in Non-Equilibrium Magnetized Plasma: The Role of Plasma Kinetics

Anna V. Bogatskaya [1,2,*] **, Nelli E. Gnezdovskaia** [1] **and Alexander M. Popov** [1,2]

[1] Department of Physics, Moscow State University, 119991 Moscow, Russia;
    gnezdovsky.ne15@physics.msu.ru (N.E.G.); popov@mics.msu.su (A.M.P.)
[2] P. N. Lebedev Physical Institute, RAS, 119991 Moscow, Russia
* Correspondence: abogatskaya@mics.msu.su; Tel.: +7-495-939-4954

check for
updates

Abstract: In this paper the theoretical model to consider the influence of kinetic properties of nonequilibrium two-color plasma during the THz pulses generation in the presence of static magnetic field is developed. It is shown that applying a static magnetic field on a gas along the direction of propagation of an ionizing two-color laser pulse allows one to produce two-frequency emissions in THz range with tunable central frequency and bandwidth, which are strongly dependent on electron velocity distribution function (EVDF) formed in the plasma as well as relations between collisional, plasma and cyclotron frequencies.

1. Introduction

The continuing interest over the years in sources of terahertz radiation is caused by their manifold applications in various fields, such as spectroscopy, material science, biology, medicine, security systems and so on [1–5]. Among the plasma-based methods of THz generation two-color schemes providing strong THz pulses with a very broad spectrum are the most popular [6–11]. In addition to the interest in increasing the peak power of generated THz pulses [12–14], their tunability as well as polarization are also of great importance as they provide an additional degree of freedom to control pulses and their interactions with matter [15]. For example, elliptically or circularly polarized THz waves are potentially important for polarization-dependent terahertz spectroscopy, i.e., studying macromolecular chiral structures, such as proteins and DNA [16–19]. There are different electro-optical methods to generate THz with tunable polarization, among them are the managing of phases and polarizations of two-color pump pulses [11,20,21], using double helix electrodes [22]. The other way is to produce elliptically polarized THz pulses from magnetized gas plasmas by changing the external magnetic field strength [23,24].

In this paper a comprehensive theoretical consideration of the kinetic effect of nonequilibrium plasma formed by two-color laser pulses in the presence of static magnetic field on the process of THz pulses emission is developed. In [24] it was predicted that by introducing static magnetic field one can switch from a source emitting at an only plasma frequency ω_p to a dual-frequency emitter: one above ω_p (or even near the cyclotron frequency ω_B) and the other below it. Thus, it was demonstrated that the presence of magnetic field provides tunability in central frequency and polarization of generated THz pulses which seems to be very perspective. However, all the results in [24] were done under the assumption of collisionless plasma. The novelty of the current research lies in the demonstration of the fact that accounting of plasma kinetics during the elastic collisions causes the essential variation of the spectral characteristics of generated pulse thus leading to a change in signal duration. It will be shown

that by applying static magnetic field, we are able to produce two-frequency tunable THz source with varying bandwidth which is sensitive to the velocity distribution function as well as the velocity dependence of the transport cross section in gas. Recently such a theoretical study was done for the case of nonmagnetic nonequilibrium two-color plasma [25] based on the dispersive equation solution for longitudinal oscillations within the framework of elementary and kinetic models of plasma volume. The principal scheme we are going to consider is presented in Figure 1. A two-color high-intense laser pulse ionizes the gas target and creates a rather dense plasma within the region of the laser focal waist. A static magnetic field B_0 is applied along the plasma formation direction.
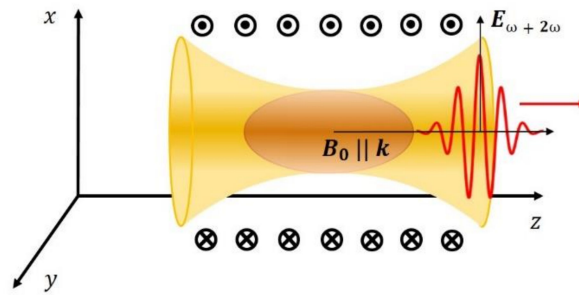

Figure 1. Principal scheme of plasma formation by two-color laser pulse. Static magnetic field is assumed to be along the plasma volume formed by the ionizing femtosecond two-color pulse.

2. Models and Main Equations

2.1. THz Emission from Two-Color Plasma in the Presence of Static Magnetic Field: Elementary Model

To consider the THz emission here we assume that plasma is formed by two-color Ti-Sa (or some other fundamental wavelength) laser pulse with the sine-squared envelope consisting of linearly polarized fundamental and second harmonics. The intensity of fundamental harmonic is about $3.3 \cdot 10^{13}$ W/cm^2 (for the 2nd harmonic this value was four times less), pulse duration is about 100 fs, phase shift between the harmonics is $\pi/2$. Under the action of such a pulse as a result of tunnel ionization of atoms [26,27] the plasma with ionization degree of about $2.7 \cdot 10^{-4}$ can be formed which leads to the electron concentration about $N_e \cong 7 \cdot 10^{15}$ cm^{-3} [25]. Here we suppose that during the fs-laser pulse action the gas temperature doesn't change. It is not necessary to specify the gas within the elementary model of plasma electrons, but further we will perform our simulations for the gas xenon due to its fast-growing energy dependence of transport scattering cross section in order to show the essential influence of kinetic properties on the THz pulses formation.

From [6,7] it is known that the asymmetry of the ionization process under the two-color pulse action leads to the formation of longitudinal plasma oscillations. To obtain the frequency domain and decay rate of these oscillations one should solve the dispersive equation for longitudinal plasma waves:

$$0 = \frac{\omega^2}{c^2} \varepsilon(\omega), \tag{1}$$

where $\varepsilon(\omega) = 1 + i\frac{4\pi\sigma(\omega)}{\omega}$ is the plasma permittivity at frequency ω and $\sigma(\omega)$ is the plasma conductivity. It should be mentioned that equation (1) is written for the longitudinal waves in free space. Considering the geometry of limited volume of the plasma formation, the geometrical factor of depolarization η should be introduced (see [28]). Then Equation (1) can be rewritten as [28]:

$$0 = \frac{\omega^2}{c^2}(1 + \eta(\varepsilon(\omega) - 1)). \tag{2}$$

For the spherical plasma volume depolarization factor $\eta = 1/3$, in the case of the cylindrical geometry (the electric field vector is perpendicular to the axis) $\eta = 1/2$. If the length of plasma

formation is larger than its diameter the value for cylindrical geometry can also be used. Hence further we suppose that $\eta \approx 1/2$. From Equation (2) one obtains the relation for the longitudinal plasma waves $\varepsilon = 1 - 1/\eta \approx 1/2$. Taking into account that plasma conductivity is $\sigma(\omega) = e^2 N_e / m(v_{tr} - i\omega)$ (here v_{tr} denotes the transport collisional frequency of electrons and N_e is electron density in plasma) one obtains the following expression for resonance frequency [27]:

$$\omega = \sqrt{\omega_p^2/2 - \frac{v_{tr}^2}{4}} - i\frac{v_{tr}}{2}. \tag{3}$$

Here $\omega_p = \sqrt{\frac{4\pi e^2 N_e}{m}}$ is the plasma frequency. If the parameter $\frac{v_{tr}}{\omega_p} < 1$ one obtains from (3):

$$\omega \approx \frac{\omega_p}{\sqrt{2}} - i\frac{v_{tr}}{2}. \tag{4}$$

For the laser plasma parameters mentioned in the beginning of this Section the longitudinal plasma oscillations occur in the THz frequency band and, hence, can produce THz radiation at frequency $\omega_p/\sqrt{2}$ while v_{tr} defines the THz pulse duration. The key issue of the current research is the study of plasma emission occurring in the presence of the external magnetic field. In this case the situation is essentially different. Further we will study the geometry when the wave vector of the laser pulse is collinear to the external magnetic field directed along *z*-axis (see Figure 1). In such a geometry plasma electrons created by the two-color laser pulse oscillate in xy–plane. Thereby the electron motion can be represented as a superposition of two counter-rotating waves. The external static magnetic field directed along *z*-axis splits the longitudinal plasma oscillations into two branches which can generate circularly polarized THz pulses at different frequencies.

To provide more insight into the electron motion in magnetized plasma let us write the equation for the electron motion assuming the cylindrical plasma geometry in a form:

$$\ddot{\vec{r}} + v_{tr}\dot{\vec{r}} + \omega_p^2/2 \cdot \vec{r} = e/mc \cdot \dot{\vec{r}} \times \vec{B_0}, \tag{5}$$

Here we suppose that the magnetic field induction $\vec{B_0}$ vector is directed along *z*-axis and plasma oscillations appear to exist in xy-plane. Introducing new variables $\xi = (x + iy)/\sqrt{2}$ and $\eta = (x - iy)/\sqrt{2}$ we obtain the following solution of Equation (5):

$$\xi \sim \exp(-i\omega_- t), \tag{6}$$

$$\eta \sim \exp(-i\omega_+ t), \tag{7}$$

where:

$$\omega_\pm = -\frac{(\pm\omega_B + iv_{tr})}{2} + \sqrt{\frac{\omega_B^2 - v_{tr}^2 \pm 2i\omega_B v_{tr}}{4} + \frac{\omega_p^2}{2}}, \tag{8}$$

(here $\omega_B = eB_0/mc$ is the cyclotron frequency) corresponding to the rotation of the plasma electrons at opposite directions with two different frequencies. Such rotational motion will result in circularly polarized THz emission.

For further consideration we introduce the plasma conductivity tensor (see, for example, [29]). In the geometry under the study the components of conductivity tensor are given by the expression:

$$\sigma(\omega) = e^2 N_e / m(v_{tr} - i(\omega \pm \omega_B))., \tag{9}$$

In [24] it was shown that the presence of magnetic field along the propagation direction of a two-color laser pulse enables to produce circularly polarized terahertz radiation with tunable central frequency and spectral width.

Really, by considering the cylindrical shape of plasma formation (this seems to be the closest to the real shape of laser focal waist) and thus substituting $\eta = 1/2$ into (2) one derives the following equation for longitudinal plasma waves:

$$\omega = \frac{1}{2}\omega_p^2 \frac{1}{(\omega \pm \omega_B) + i\nu_{tr}}, \tag{10}$$

The solution of Equation (10) that makes physical sense provides the frequencies corresponding to expression (8).

As it was mentioned before the magnetic field allows two branches of solution: with the lower and the higher central frequency. The lower frequency solution (ω_+) corresponds to the «+» sign in Equation (10), the higher frequency (ω_-) is for the «-» sign. One can also see that for the case of nonmagnetic plasma solution (8) is reduced to the Formula (3). It will be further demonstrated that the higher frequency solution branch can take values in the range from ω_p to more than ω_B and, hence, can be varied depending on the static magnetic field value. The collisional bandwidth of the solution branches is determined by the ratios of the plasma parameters ($\omega_p, \nu_{tr}(\nu)$) as well as the cyclotron frequency. In the simplest case of collisionless plasma the solution (8) reduces to:

$$\omega_\pm = \mp\frac{\omega_B}{2} + \sqrt{\frac{\omega_B^2}{4} + \frac{\omega_p^2}{2}}, \tag{11}$$

and is in agreement with [24].

If the magnetic field is weak enough $\omega_B \ll \omega_p$, from Equation (8) one obtains:

$$\omega_\pm \approx \omega_p / \sqrt{2} \mp \omega_B/2 - i\nu_{tr}/2. \tag{12}$$

The splitting is small (we note that in some sense this expression is similar to that obtained for the classical model of Zeeman splitting) and the relaxation time is the same for both wave branches.

Let us consider the case of large cyclotron frequency: $\omega_B \gg \omega_p \gg \nu_{tr}$. Then the general solution (8) is divided into the following branches:

$$\omega_- \approx \omega_B + \frac{\omega_p^2}{2\omega_B} - i\nu_{tr}, \tag{13}$$

$$\omega_+ \approx \frac{\omega_p^2}{2\omega_B} - i\nu_{tr}\frac{\omega_p^2}{2\omega_B^2}. \tag{14}$$

One can see that by varying the induction of magnetic field it is possible to adjust the carrier frequency of plasma oscillations independently from the plasma electron density and two-color laser pulse intensity. We also show that the high-frequency branch of plasma oscillations (13) has faster attenuation rate (larger imaginary part) than low-frequency solution (14). It means that such a plasma under the influence of magnetic field appears to be two-frequency tunable emission source in THz range with different durations (or bandwidth) of generated pulses.

2.2. THz Emission of Two-Color Plasma in the Presence of Static Magnetic Field: Kinetic Model of Plasma

The main issue of the current Section is the study of plasma kinetic effect on the process of tunable THz pulse formation in magnetized nonequilibrium plasma. In the model described above it was supposed that the transport frequency has constant value. In reality this value is the function of electron velocity that can essentially vary for different gases. Hence, plasma properties will depend

on the velocity distribution of electrons and plasma wave formation should be analyzed within the kinetic approach based on the kinetic Boltzmann equation. Within the framework of the two-term expansion for Boltzmann kinetic equation the plasma conductivity in the presence of magnetic field can be expressed as [29,30]:

$$\sigma(\omega) = \frac{\omega_p^2}{3} \int_0^\infty \frac{v^3(v_{tr}(v) + i(\omega \pm \omega_B))}{(\omega \pm \omega_B)^2 + v_{tr}^2(v)} \left(-\frac{\partial f}{\partial v}\right) dv, \tag{15}$$

where $f(v)$ stands for electron distribution function over absolute value of velocity (EVDF) normalized by $\int_0^\infty f(v)v^2 dv = 1/4\pi$. Substituting (15) in dispersive Equation (2) for the cylindrical plasma geometry one obtains the following integral equation for the frequency of longitudinal plasma oscillations:

$$\omega = \frac{1}{2}\frac{4\pi}{3}\omega_p^2 \int_0^\infty \frac{v^3((\omega \pm \omega_B) - iv_{tr}(v))}{(\omega \pm \omega_B)^2 + v_{tr}^2(v)} \left(-\frac{\partial f}{\partial v}\right) dv. \tag{16}$$

The solution of the Equation (16) provides the spectrum of plasma waves for the given electron velocity distribution function (EVDF) and in general terms should be solved numerically. Below we are going to analyze some limiting cases which can be resolved analytically under the assumption that EVDF remains stationary while the emission from plasma takes place. Let us first consider «+» sign in Equation (16). In this case it is wise to neglect the $v_{tr}^2(v)$ term in denominator and thus solution of (16) will be:

$$\omega_+ \approx \frac{\omega_p^2}{2\omega_B} - i\frac{\omega_p^2}{2\omega_B^2}\left[\langle v_{tr}\rangle + \frac{1}{3}\langle v\frac{\partial v_{tr}(v)}{\partial v}\rangle\right]. \tag{17}$$

Here $\langle\rangle$ means averaging over the electron velocity distribution function in plasma. The above solution is correlated with the solution (14) within the elementary theory and stands for the low-frequency branch of plasma waves.

When considering the «-» sign in Equation (16) two possible branches can occur: $|\omega - \omega_B| \ll \langle v_{tr}\rangle$ or $|\omega - \omega_B| \gg \langle v_{tr}\rangle$. If $|\omega - \omega_B| \gg \langle v_{tr}\rangle$ the solution reads:

$$\omega_- \approx \omega_B + \frac{\omega_p^2}{2\omega_B} - i\left[\langle v_{tr}\rangle + \frac{1}{3}\langle v\frac{\partial v_{tr}(v)}{\partial v}\rangle\right]. \tag{18}$$

Here one should also demand that $\langle v_{tr}\rangle \ll \frac{\omega_p^2}{2\omega_B}$ for the above-mentioned parameters. It means that the achievement/non-achievement of this condition generally depends on the given dependence of transport scattering cross section and given electron velocity distribution function. Some specific EVDFs which are formed in xenon under the two-color laser pulse action will be discussed in the next Section. It can be seen from solutions (17), (18) that accounting of plasma kinetics leads to the additional term $\frac{1}{3}\langle v\frac{\partial v_{tr}(v)}{\partial v}\rangle$ in the imaginary part compared to elementary model (13), (14) which could be both positive or negative depending on the sign of the derivative $\frac{\partial v_{tr}(v)}{\partial v}$ in the velocity range where it contributes mainly to the integration over EVDF. A similar term was obtained in [27] for the case of non-magnetized plasma. Thus, taking into account both the velocity dependence of transport scattering cross section and distribution of electrons enables to describe the spectrum of emitted radiation from plasma more correctly.

The most interesting case occurs near the cyclotron resonance when $|\omega - \omega_B| \ll \langle v_{tr}\rangle$. In this case neglecting the term $(\omega - \omega_B)^2$ in denominator (16) the solution will be:

$$\omega_- \approx \omega_B\frac{\omega_p^2/2\cdot\xi}{\omega_p^2/2\cdot\xi - 1} - i\frac{\omega_p^2}{2}\left[\langle\frac{1}{v_{tr}}\rangle - \frac{1}{3}\langle\frac{v}{v_{tr}^2}\frac{\partial v_{tr}(v)}{\partial v}\rangle\right], \tag{19}$$

where $\xi = \langle\frac{1}{v_{tr}^2}\rangle - \frac{2}{3}\langle\frac{v}{v_{tr}^3}\frac{\partial v_{tr}(v)}{\partial v}\rangle$. If $\omega_p^2/2\cdot\xi \gg 1$ the real part of (19) is found to be close to ω_B. It should be noted that this case is beyond the elementary model of plasma as it is impossible to accomplish there the condition $\omega_p^2/2\cdot\xi \gg 1$ together with $|\omega - \omega_B| \sim \omega_p^2/2\cdot\langle 1/v_{tr}\rangle \ll \langle v_{tr}\rangle$. Indeed, as within the elementary model $\langle v_{tr}\rangle = v_{tr}, \langle 1/v_{tr}\rangle = 1/v_{tr}, \langle 1/v_{tr}^2\rangle = 1/v_{tr}^2$, the first mentioned condition reduces to the $\omega_p \gg v_{tr}$, while the second condition goes to the opposite one: $\omega_p \ll v_{tr}$.

3. Results and Discussion

3.1. Different Kinds of Electron Energy Distribution Functions Formed under the Action of Two-Color Laser Pulses

In this Section we would like to analyse a number of nonequilibrium electron velocity distribution functions formed in xenon plasma by two-color laser pulses and their evolution [27]. Figure 2 demonstrates EVDFs formed along the polarization axis during the tunnel ionization of xenon by two-color femtosecond laser pulses with fundamental wavelengths of 800 and 3900 nm. Both obtained distributions are highly nonequilibrium and have sharp angular distribution along the direction of the pulse polarization. Below we will call them EVDF$_1$ for the distribution formed by the (400 + 800) nm laser pulse and EVDF$_2$ for the distribution formed by the (1950 + 3900) nm laser pulse. According to the plasma kinetic theory, elastic collisions lead to the isotropization of angular distribution of electrons, while the domination of electron-electron collisions determines fast maxwellization of EVDF. Duration of the maxwellization process can be estimated as $\tau_M \sim v_{ee}^{-1}$, where v_{ee} is the frequency of electron - electron collisions. By estimating electron-electron collisional cross section as $\sigma_e^e \approx \frac{\pi e^4 L_e}{\varepsilon_e^2}$ (here ε_e is the electron energy and $L_e \approx 10$ is the Coulomb logarithm) for $\varepsilon_{e1} \sim 0.5$ eV which corresponds to maximum of EVDF$_1$ (see Figure 2) and $\varepsilon_{e2} \sim 12.4$ eV for the EVDF$_2$, one obtains $\tau_{M1} \sim 1.4 \times 10^{-11}$ s and $\tau_{M2} \sim 1.6 \times 10^{-9}$ s. For both cases N_e was chosen to be $7\cdot 10^{15}$ cm^{-3}. The above estimates lead to the fact that for the EVDF$_1$ fast Maxwellization will take place, while for the EVDF$_2$ elastic collisions will redistribute electrons rather quickly (within the time interval of several collisions) leading to the isotropic distribution in velocity space. For the transport collisional frequencies we derive $v_{tr1} \approx 10^{11}$ s^{-1} and $v_{tr2} \approx 6.6 \times 10^{12}$ s^{-1}. Thus, for the time of isotropization of EVDF$_2$ one can obtain $\tau_{is2} \approx v_{tr2}^{-1} \approx 0.15 \times 10^{-12}$ s.
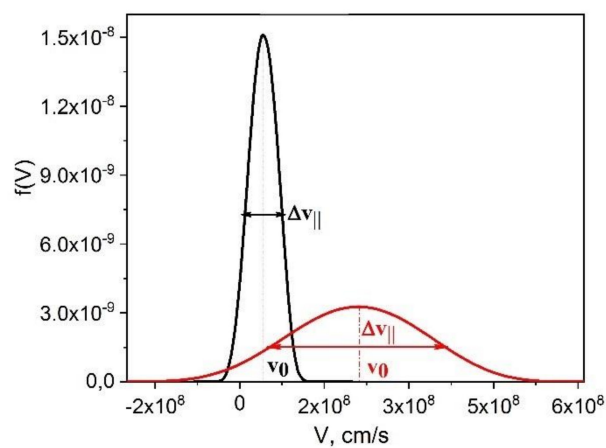

Figure 2. One-dimensional electron velocity distribution functions (EVDF) along the polarization of two-color laser field with fundamental wavelengths 800 nm (black curve) and 3900 nm (red curve). Here v_0, $\Delta v_{\parallel}$ are the mean velocity and velocity dispersion correspondingly: $v_0 = 4.2\cdot 10^7$, $\Delta v_{\parallel} = 5.3\cdot 10^7$ cm/s for 800 nm; $v_0 = 2.09\cdot 10^8$, $\Delta v_{\parallel} = 2.46\cdot 10^8$ cm/s for 3900 nm. Distribution functions are normalized to unity.

To estimate the temperature T of the maxwellized $EVDF_1$ one can write the following relation:

$$\frac{1}{2}\frac{m\left(\Delta v_\parallel\right)^2}{2} + \frac{m(v_0)^2}{2} + 2\cdot\frac{1}{2}\frac{m(\Delta v_\perp)^2}{2} = \frac{3}{2}T. \tag{20}$$

which has the sense of energy conservation law during the isotropization process in three-dimensional velocity space. Here v_0, $\Delta v_\parallel$ are taken from Figure 2, $\Delta v_\perp$ stands for the transverse distribution of photoelectrons formed in the tunnel ionization, which is estimated to be approximately equal $5.3\cdot10^7$ cm/s [27]. In Figure 3 the obtained redistributed $EVDF_{1,2}$ are plotted with the function $v\frac{\partial v_{tr}(v)}{\partial v}$ for xenon to analyse the contribution of kinetic effects to the imaginary part of solutions (17–19), which determines the collisional damping of plasma waves. The data for transport scattering cross section for xenon atom were taken from [31]. As for distribution (2) in Figure 3 it comes from the distribution formed by the (1950 + 3900) nm laser pulse replotted for the velocity module and renormalized in three-dimensional velocity space. One can see, for example, that for the distribution (2) the negative value of function $v\frac{\partial v_{tr}(v)}{\partial v}$ can decrease the value of damping coefficientthereby leading to the formation of longer THz pulses with narrower spectrum, while for the distribution (1) the term $v\frac{\partial v_{tr}(v)}{\partial v}$ is mostly positive in the area of integration.
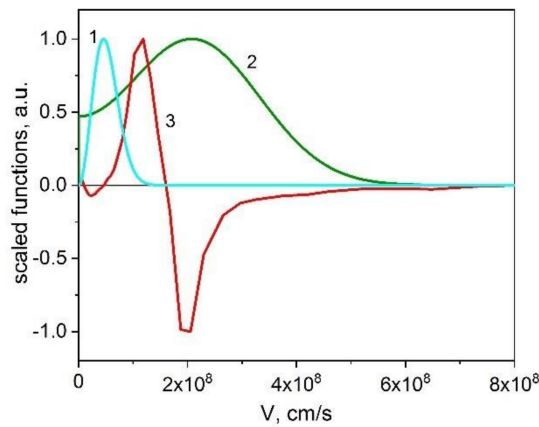

Figure 3. $EVDF_1$ after the maxwellization process (1), $EVDF_2$ after the isotropisation process (2) and $v\frac{\partial v_{tr}(v)}{\partial v}$ (3). Characteristic times of maxwellization and isotropization processes are $\tau_{M1} \sim 1.4 \times 10^{-11}$ s and $\tau_{is2} \approx 0.15 \times 10^{-12}$ s correspondingly (see the estimates above). All the functions are scaled (divided by maximum values). $EEDF_1$ and $EEDF_2$ represent the velocity distribution in three-dimensional velocity space and normalized by the condition $\int f(v)v^2dv = 1/4\pi$.

3.2. Spectral Characterictics of THz Pulses Emitted from Plasma in the Presence of Static Magnetic Field

For the simulations within this Section let us start from the elementary model of plasma and take the following parameters: plasma frequency $\omega_p = 5\cdot10^{12}$ s^{-1} (which corresponds to the electron concentration $N_e = 7\cdot10^{15}$ cm^{-3}), $v_{tr} = 10^{12}$ s^{-1} (here we selected gas xenon at atmospheric pressure and the mean velocity of electrons was chosen to be about 10^8 cm/s). The cyclotron frequency ω_B is chosen to be about $2\omega_p = 10^{13}$ s^{-1}. This corresponds to the magnetic field induction $B_0 = 6\cdot10^5$ G. Thus, the values of solutions (13), (14) for plasma wave emission in the frames of elementary model are:

$$\omega_- \approx 1.13\cdot10^{13} - i \times 10^{12} \text{ s}-^1, \tag{21}$$

$$\omega_+ \approx 1.25\cdot10^{12} - i \times 1.25\cdot10^{11} \text{ s}-^1. \tag{22}$$

In can be observed that the first solution gives high (near the cyclotron) frequency pulse, while the second one provides an order of value lower-frequency THz pulse. In both cases pulses are of about ten cycles duration.

Using the velocity distribution functions obtained in the previous section one can also find solutions of dispersive equation in the frames of the kinetic model of plasma. Further we denote the solutions related to EVFD$_1$ by the index «1» and solutions for the EVFD$_2$ by the index «2». The solution (17) representing the low-frequency branch of plasma oscillations reads:

$$\omega_+^{(1)} \approx 1.25 \cdot 10^{12} - i \times 1.58 \times 10^{11} \text{ s}^{-1}, \tag{23}$$

$$\omega_+^{(2)} \approx 1.25 \cdot 10^{12} - i \times 5.87 \cdot 10^{11} \text{ s}^{-1}. \tag{24}$$

The values (23), (24) and further results were obtained by the means of numerical integration of expressions (17), (18) and (19) over given EVDFs (see Figure 3). As it was discussed before, there is a significant influence of the plasma kinetic properties on spectral characteristics of THz signals generated from plasma. In particular, plasma with the EVDF$_1$ formed by the (400 + 800) nm laser pulse causes lower damping coefficient compared to the plasma characterized by the EVDF$_2$ (formed by the (1950 + 3900) nm laser pulse). As the damping coefficient stands for the pulse bandwidth and, as a consequence, for the pulse duration ($\frac{1}{\text{Im}\left[\omega_\pm^{(1,2)}\right]} \sim \tau_p$), in the first case longer THz pulse is assumed to be generated.

As concerns the high-frequency branch of the solution, it was demonstrated that two possible cases can take place. But in reality only one branch survives in each case. Indeed, the numerical analysis shows that the condition $\langle v_{tr} \rangle \ll \frac{\omega_p^2}{2\omega_B}$ allowing the situation $|\omega - \omega_B| \gg \langle v_{tr} \rangle$ is accomplished only for the EVFD$_1$: $\frac{\omega_p^2}{2\omega_B} = 1.3 \cdot 10^{12}$ s^{-1}, $\langle v_{tr} \rangle_{\text{EVDF1}} \approx 6.5 \times 10^{11}$ s^{-1}, $\langle v_{tr} \rangle_{\text{EVDF2}} \approx 5.3 \times 10^{12}$ s^{-1}. So, high-frequency solution branch in the form of (18) can be found for plasma characterized by EVFD$_1$:

$$\omega_-^{(1)} \approx 1.13 \cdot 10^{13} - i \times 1.26 \times 10^{12} \text{ s}^{-1}, \tag{25}$$

At the same time high-frequency solution in the form of (19) when $|\omega - \omega_B| \ll v_{tr}$ gives the following results:

$$\omega_-^{(1)} \approx 1.00 \cdot 10^{13} - i \times 4.1 \times 10^{13} \text{ s}^{-1}, \tag{26}$$

$$\omega_-^{(2)} \approx 1.04 \cdot 10^{13} - i \times 6.4 \cdot 10^{12} \text{ s}^{-1}. \tag{27}$$

From Equations (26) and (27) one can conclude that $\omega_-^{(1)}$ doesn't represent the oscillatory solution as the damping coefficient is larger than central frequency. Thus, in this case only the solution (27) for plasma with EVFD$_2$ survives.

4. Conclusions

In conclusion, we have investigated analytically and numerically the process of THz pulse emission from a nonequilibrium plasma formed by a two-color (mid)IR laser pulse in the presence of a static magnetic field. Special attention was paid to the kinetic approach to the description of plasma properties. Is was demonstrated that accounting for plasma kinetics leads to the essential variations of spectral characteristics of generated waves in plasma depending on the gas transport cross section and the specific velocity distribution function of the plasma electrons. Thus, by applying static magnetic field, we are able to produce a double-frequency THz source with tunable central frequencies determined by the value of cyclotron frequency as well as varying bandwidths which are highly sensitive to the kinetic features of plasma. Values of magnetic fields of interest (about 10^5 G) are widely available in the form of DC or pulsed magnets [32–34]. In particular, the magnet which

can be used to create suitable for our consideration magnetic field strengths is available at Institute of Applied Physics of the Russian Academy of Sciences (RAS) [35].

Conflicts of Interest: The authors declare no conflict of interest.

References

1. Tonouchi, M. Cutting-Edge Terahertz Technology. *Nat. Photonics* **2007**, *1*, 97–105. [CrossRef]
2. Nagai, N.; Sumitomo, M.; Imaizumi, M.; Fukasawa, R. Characterization of electron- or proton-irradiated Si space solar cells by THz spectroscopy. *Semicond. Sci. Technol.* **2006**, *21*, 201. [CrossRef]
3. Liu, J.; Dai, J.; Chin, S.L.; Zhang, X.; Broadband, C. Terahertz wave remote sensing using coherent manipulation of fluorescence from asymmetrically ionized gases. *Nat. Photonics* **2010**, *4*, 627. [CrossRef]
4. Fischer, B.M.; Walther, M.; Jepsen, P.U. Far-infrared vibrational modes of DNA components studied by terahertz time-domain spectroscopy. *Phys. Med. Biol.* **2002**, *47*, 3807. [CrossRef]
5. Kampfrath, T.; Tanaka, K.; Nelson, K.A. Resonant and nonresonant control over matter and light by intense terahertz transients. *Nat. Photonics* **2013**, *7*, 680. [CrossRef]
6. Kim, K.Y.; Glownia, J.H.; Taylor, A.; Rodriguez, J.G. Terahertz emission from ultrafast ionizing air in symmetry-broken laser fields. *Opt. Express* **2007**, *15*, 4577. [CrossRef]
7. Gildenburg, V.B.; Vvedenskii, N.V. Optical-to-THz Wave Conversion via Excitation of Plasma Oscillations in the Tunneling-Ionization Process. *Phys. Rev. Lett.* **2007**, *98*, 245002. [CrossRef]
8. Thomson, M.D.; Blank, V.; Roskos, H.G. Terahertz white-light pulses from an air plasma photo-induced by incommensurate two-color optical fields. *Opt. Express* **2010**, *18*, 23173. [CrossRef]
9. Clerici, M.; Peccianti, M.; Schmidt, B.E.; Caspani, L.; Shalaby, M.; Giguère, M.; Lotti, A.; Couairon, A.; Légaré, F.; Ozaki, T.; et al. Wavelength scaling of terahertz generation by gas ionization. *Phys. Rev. Lett.* **2013**, *110*, 253901. [CrossRef]
10. Oh, T.I.; Yoo, Y.J.; You, Y.S.; Kim, K.Y. Generation of strong terahertz fields exceeding 8 MV/cm at 1 kHz and real-time beam profiling. *Appl. Phys. Lett.* **2014**, *105*, 041103. [CrossRef]
11. Kosareva, O.; Esaulkov, M.; Panov, N.; Andreeva, V.; Shipilo, D.; Solyankin, P.; Demircan, A.; Babushkin, I.; Makarov, V.; Morgner, U.; et al. Polarization control of terahertz radiation from two-color femtosecond gas breakdown plasma. *Opt. Lett.* **2018**, *43*, 90–93. [CrossRef] [PubMed]
12. Bogatskaya, A.V.; Smetanin, I.V.; Volkova, E.A.; Popov, A.M. Guiding and amplification of microwave radiation in a plasma channel created in gas by intense ultraviolet laser pulse. *Laser Part. Beams* **2015**, *33*, 17–25. [CrossRef]
13. Bogatskaya, A.V.; Popov, A.M. New approach to the problem of thz generation by intense two-color laser fields. *Laser Phys.* **2018**, *28*, 115301. [CrossRef]
14. Bogatskaya, A.V.; Popov, A.M. Resonance-enhanced thz generation from aluminium vapour irradiated by ti–sa laser pulse and its second harmonic. *Laser Phys. Lett.* **2018**, *15*, 105301. [CrossRef]
15. Shan, J.; Dadap, J.I.; Heinz, T.F. Circularly polarized light in the single-cycle limit: The nature of highly polychromatic radiation of defined polarization. *Opt. Express* **2009**, *17*, 7431–7439. [CrossRef] [PubMed]
16. Katletz, S.; Pfleger, M.; Pühringer, H.; Mikulics, M.; Vieweg, N.; Peters, O.; Scherger, B.; Scheller, M.; Koch, M.; Wiesauer, K. Polarization sensitive terahertz imaging: Detection of birefringence and optical axis. *Opt. Express* **2012**, *20*, 23025–23035. [CrossRef]
17. Zhang, P.; Su, F.; Zhang, S.; Mei, H.; Zhang, C.; Luo, X.; Dai, J.; Pi, L. Terahertz magnetic circular dichroism induced by exchange resonance in $CoCr_2O_4$ single crystal. *Opt. Express* **2015**, *23*, 17805–17814. [CrossRef]
18. Wang, X.; Cui, Y.; Sun, W.; Ye, J.; Zhang, Y. Terahertz polarization real-time imaging based on balanced electro-optic detection. *J. Opt. Soc. Am. A* **2010**, *27*, 2387–2393. [CrossRef]

19. Nagai, M.; Nakane, A.; Suzukawa, H.; Morimoto, T.; Ashida, M. Time-Domain Magnetic Field-Difference Spectroscopy for Semiconductors Using Circularly Polarized Terahertz Pulses. *IEEE Trans. Terahertz Sci. Technol.* **2020**, 51–57. [CrossRef]

20. Wen, H.; Lindenberg, A.M. Coherent Terahertz Polarization Control through Manipulation of Electron Trajectories. *Phys. Rev. Lett.* **2009**, *103*, 119903. [CrossRef]

21. Jianming, D.; Karpowicz, N.; Zhang, X.-C. Coherent Polarization Control of Terahertz Waves Generated from Two-Color Laser-Induced Gas Plasma. *Phys. Rev. Lett.* **2009**, *103*, 023001. [CrossRef]

22. Lu, X.; Zhang, X.-C. Generation of Elliptically Polarized Terahertz Waves from Laser-Induced Plasma with Double Helix Electrodes. *Phys. Rev. Lett.* **2012**, *108*, 123903. [CrossRef] [PubMed]

23. Liu, C.S.; Tripathi, V.K. Tunable terahertz radiation from a tunnel ionized magnetized plasma cylinder. *J. Appl. Phys.* **2009**, *105*, 013313. [CrossRef]

24. Wang, W.-M.; Gibbon, P.; Sheng, Z.-M.; Li, Y.-T. Tunable Circularly Polarized Terahertz Radiation from Magnetized Gas Plasma. *Phys. Rev. Lett.* **2014**, *114*, 253901. [CrossRef] [PubMed]

25. Bogatskaya, A.V.; Gnezdovskaia, N.E.; Popov, A.M. The role of plasma kinetic processes during high intense thz pulses generation. In Proceedings of the 8th International Conference on Photonics, Optics and Laser Technology, Valletta, Malta, 27–29 February 2020.

26. Delone, N.B.; Krainov, V.P. Tunneling and barrier-suppression ionization of atoms and ions in a laser radiation field. *Phys. Usp.* **1998**, *41*, 469. [CrossRef]

27. Tong, X.M.; Lin, C.D. Empirical formula for static field ionization rates of atoms and molecules by lasers in the barrier-suppression regime. *J. Phys. B* **2005**, *38*, 2593. [CrossRef]

28. Landau, L.D.; Lifshitz, E.M.; Pitaevskii, L.P. *Electrodynamics of Continuous Media*, 2nd ed.; Butterworth Heinemann: Oxford, UK, 1984.

29. Ginzburg, V.L.; Gurevich, A.V. Nonlinear phenomena in a Plasma located in an alternating electromagnetic field. *Sov. Phys. Usp.* **1960**, *3*, 115–146. [CrossRef]

30. Raizer, Y.P. *Laser-Induced Discharge Phenomena*; Consultants Bureau: New York, NY, USA, 1974.

31. Hayashi, M. Determination of electron-xenon total excitation cross-sections, from threshold to 100 eV, from experimental values of Townsend's α. *J. Phys. D* **1983**, *16*, 581. [CrossRef]

32. Matsuda, Y.H.; Herlach, F.; Ikeda, S.; Miura, N. Generation of 600 T by electromagnetic flux compression with improved implosion symmetry. *Rev. Sci. Instrum.* **2002**, *73*, 4288–4294. [CrossRef]

33. Portugall, O.; Puhlmann, N.; Muller, H.U.; Barczewski, M.; Stolpe, I.; von Ortenberg, M. Megagauss magnetic field generation in single-turn coils: New frontiers for scientific experiments. *J. Phys. D Appl. Phys.* **1999**, *32*, 2354–2366. [CrossRef]

34. Hahn, S.; Kim, K.; Kim, K.; Hu, X.; Painter, T.; Dixon, I.; Kim, S.; Bhattarai, K.R.; Noguchi, S.; Jaroszynski, J.; et al. 45.5-tesla direct-current magnetic field generated with a high-temperature superconducting magnet. *Nature* **2019**, *570*, 496–499. [CrossRef] [PubMed]

35. High Field Research Magnet. Available online: https://www.jastec-inc.com/e_top/ (accessed on 23 September 2020).